

## Regular article

# Understanding the anomalous thermal behavior of $\Sigma 3$ grain boundaries in a variety of FCC metals

Ian Chesser, Elizabeth Holm\*

Department of Materials Science and Engineering, Carnegie Mellon University, 5000 Forbes Avenue Wean Hall 3325, Pittsburgh, PA 15213, United States of America

## ARTICLE INFO

## Article history:

Received 3 May 2018

Received in revised form 20 June 2018

Accepted 9 July 2018

Available online xxxx

## Keywords:

Grain boundaries

Molecular dynamics (MD)

Thermally activated processes

Twinning

Activation energy

## ABSTRACT

We present a case study of the complex temperature dependence of grain boundary mobility. The same general incoherent twin boundary in different FCC metals is found to display antithermal, thermal, and mixed mobility during molecular dynamics synthetic driving force simulations. A recently developed energy metric known as the generalized interfacial fault energy (GIFE) surface is used to show that twin boundaries moving in an antithermal manner have a lower energetic barrier to motion than twin boundaries moving in a thermally activated manner. Predicting the temperature dependence of grain boundary motion with GIFE curves stands to accelerate research in grain boundary science.

© 2018 Elsevier Ltd. All rights reserved.

Predicting the rate at which a grain boundary moves under an applied driving force is a complex problem eminently relevant to the design of ceramic and metallic microstructures. Grain boundary mobility is defined via linearized reaction rate theory as the proportionality constant between an applied driving force and resultant grain boundary velocity [1,2]:

$$v = MP \quad (1)$$

where  $P$  is an applied driving force with units of energy density or equivalently pressure,  $v$  is grain boundary velocity, and  $M$  is mobility. Grain boundary motion is often considered to have an ideal Arrhenius temperature dependence on mobility [3]:

$$M = M_0 \exp\left(\frac{-E_a}{k_b T}\right) \quad (2)$$

$M$  is the steady state mobility,  $M_0$  is a prefactor related to the attempt frequency of grain boundary motion,  $E_a$  is an activation

energy that represents the energetic barrier to grain boundary motion, and  $k_b T$  is the thermal energy of the system. The diverse temperature dependence of grain boundary mobility in simulations and experiments implies that Eq. (2) is a vast oversimplification [1,3–9].

Molecular dynamics (MD) simulations have shown that grain boundaries frequently deviate from an ideal Arrhenius temperature dependence of mobility. Eighty-nine grain boundaries in the 388 boundary mobility survey by Olmsted et al. showed antithermal mobility over some temperature range [6,10]. Antithermal interface motion is characterized by a decrease in interface mobility with increasing temperature. It is speculated to be important to *cold fast* processes such as room temperature grain growth in nanocrystalline metals, and is experimentally observed in *hot slow* grain growth in ceramic materials like SrTiO<sub>3</sub> [3,11–13]. Understanding antithermal grain boundary motion is related to many other open problems in interface mobility, including stress driven grain growth and rotation at cryogenic temperatures, twinning and de-twinning processes, and twin defect interactions [14–19].

$\Sigma 3$  twin-related boundaries comprise over half of the antithermal boundaries in the Olmsted survey [6]. Remarkably, twin boundary mobility spans several orders of magnitude in MD simulations and shows antithermal, thermal, or mixed dependence on temperature as a function of boundary plane crystallography [20]. Previous MD mobility simulations have only considered twin boundary mobility in Ni. In this study, we consider the mobility of the same general twin boundary in twelve different FCC metals, testing fifteen interatomic potentials in total, four for Ni.

\* Corresponding author.

E-mail addresses: [ichesser@andrew.cmu.edu](mailto:ichesser@andrew.cmu.edu) (I. Chesser), [eaholm@andrew.cmu.edu](mailto:eaholm@andrew.cmu.edu) (E. Holm).

We examine the motion of a general  $\Sigma 3$   $[111] 60^\circ(11\ 8\ 5)$  grain boundary. The boundary plane is projected on the  $\Sigma 3$  grain boundary fundamental zone in Fig. 1(a). The boundary facets into segments of coherent twin (CT) and incoherent twin (ICT) boundary upon energy minimization, consistent with existing faceting models for  $\Sigma 3$  boundaries [21]. The grain boundary moves via the glide of the incoherent  $\{110\}$  facets, as shown in Fig. 1(b). The grain boundary has mixed tilt and twist character, and is most simply viewed as a rotation from the CT with  $\{111\}$  boundary planes by  $17^\circ$  about a  $\langle 112 \rangle$  axis.

Twin boundary mobility is examined with the ECO synthetic driving force (SDF) molecular dynamics method [22,23] for twelve different embedded atom method (EAM) potentials fit by Sheng et al. [24]. The Sheng potentials were fit to a variety of elemental properties, including lattice dynamics, mechanical and thermal properties, and the energetics of competing crystal structures, defects, deformation paths, and liquid structures. Three Ni potentials are considered other than the Sheng potential, including the Foiles-Hoyt Ni potential used in prior studies of antithermal grain boundary motion, the Mishin Farkas Ni potential, and the Mendeleev Ni potential [24–27]. We use the following shorthand for Ni potentials in this work: Ni1 = Sheng, Ni2 = Foiles-Hoyt, Ni3 = Mendeleev, Ni4 = Mishin/Farkas.

Grain boundaries are constructed in a simulation box in LAMMPS with periodic boundary conditions, and are minimized via a standard conjugate gradient minimization at 0 K [28]. All SDF simulations are run in an NPT ensemble with periodic boundary conditions along the grain boundary plane and free surface boundary conditions normal to the cut plane. Temperature is set with a Nose Hoover thermostat and pressures are maintained near zero along the grain boundary plane with a Parrinello Rahman barostat. A timestep of 2 fs is used to anneal grain boundaries for 0.4 ns before the synthetic driving force is turned on for 1 ns. The SDF method imposes a driving force for boundary motion in a bi-crystal by lowering the free energy of one grain and raising the free energy of the other, causing the low energy grain to grow at the expense of the high energy grain. Boundary position is tracked via the change in order parameter of a fixed region encompassing the shrinking grain. Velocity is computed as the slope of the position-time curve via the bootstrap resampling technique of Race et al. with a smoothing window of 5 ps and a sample window of 20 ps [29]. Finally, mobility is calculated in the linear approximation as velocity divided by the applied driving force.

For mobility results for different FCC metals, a driving force of 10 meV/atom was used. Previous simulations have found 1 meV/atom to be an optimal driving force for studying the motion of anti-thermal twin boundaries in Ni, since mobility values at 1 meV match values calculated in the zero driving force limit from the random walk method [30]. We choose a larger driving force because of the need to generate as much motion as possible in slow moving thermal boundaries over a 1 ns time span. We compare driven motion of Ni potentials

using a SDF of 1 meV/atom, consistent with previous studies. Note that system size is relevant to energy and mobility convergence because defects can interact across periodic boundaries and modify minimum energy structures and grain boundary dynamics [31–33]. A full justification of simulation box lengths with respect to energy and mobility can be found in the work of Humberson and Holm [31,34,35].

The mobility behavior of the same general twin boundary is found to vary with FCC metal, both across EAM potentials for different FCC metals and within EAM potentials for Ni. Fig. 2a plots mobility of the  $\Sigma 3$   $[111] 60^\circ(11\ 8\ 5)$  boundary for a variety of FCC metals with different stacking fault energies. Mobility is plotted at three homologous temperatures  $T_H$  for each metal for a synthetic driving force of 10 meV/atom. The colored background of Fig. 2a shows the clustering of FCC metals by mobility type as a function of stacking fault energy. Ca, Sr, Au, Ag, and Cu show antithermal behavior (red) while Pb, Ce, Al, Pt, and Rh show thermal behavior (blue). Pd displays mixed behavior (purple), with the intermediate temperature corresponding to the highest mobility. Although stacking fault energy is a convenient parametrization of these metals and transitions, it is not a predictor of mobility type.

Boundary mobility also varies significantly among Ni potentials, as shown in Fig. 2b. Ni4 exhibits a weakly thermal trend, while other Ni potentials show overall antithermal trends. Ni2 and Ni4, which have the same measured stacking fault energy, show different mobility type. The goal of the remainder of this work is to rationalize differences in mobility type for the same twin boundary in different FCC EAM potentials in the context of grain boundary structure and energetics.

The initial ICT facet length structure of the  $\{11\ 8\ 5\}$  boundary varies with interatomic potential. Representative facet structures are shown in Fig. 3 after a 0.4 ns anneal and a small amount of motion under a SDF. In Cu, a single facet is present with height  $15a_{(111)}$ , referred to here as  $h(15)$  following the convention of Hirth [36]. In Pb and Al, multiple facets are present after annealing. From left to right, Pb has a facet height distribution of  $\{h(6), h(9)\}$ , while Al has a facet height distribution of  $\{h(3), h(9), h(3)\}$ .

The  $h(3)$  facet is the fundamental motion unit during  $\{11\ 8\ 5\}$  boundary motion.  $h(3)$  facets can coalesce during boundary motion, presumably to reduce corner energy at facet junctions [37–39]. All elements that show anti-thermal motion show a single facet after annealing. Although most thermal boundaries retain multiple facets, Pb, Ce, and Ni4 have facets of height  $h(15)$  after annealing yet move in a thermal manner. Facet coalescence is a necessary but insufficient condition for anti-thermal motion in these simulations.

Since facet structure does not distinguish mobility type, we instead consider energy metrics relevant to twin related boundaries. A twinned crystal can be created by applying successive shearing operations to a perfect crystal. Starting with a perfect crystal block, a stacking fault is generated by applying a rigid translation of the

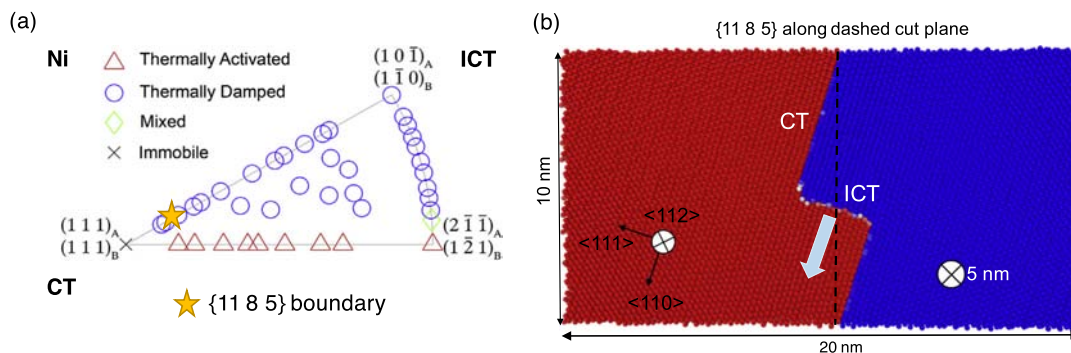


Fig. 1. (a) Boundary plane fundamental zone with points colored by mobility type [20]. The  $\{11\ 8\ 5\}$  boundary in this work is shown with a yellow star. (b) Faceted  $\{11\ 8\ 5\}$  grain boundary, schematically showing the growth of the blue grain under an energy jump driving force.

Download English Version:

<https://daneshyari.com/en/article/7909839>

Download Persian Version:

<https://daneshyari.com/article/7909839>

[Daneshyari.com](https://daneshyari.com)